Journal of the Serbian Chemical Society
JSCS@tmf.bg.ac.rs • www.shd.org.rs/JSCS
J. Serb. Chem. Soc. *88* (12) 1237–1252 (2023)
JSCS–5692
Original scientific paper
Published 19 December 2023

Spectroscopic and structural characterization of hexaamminecobalt(III) dibromide permanganate

BERTA BARTA HOLLÓ[1#], NILOOFAR BAYAT[2,3], LAURA BERECZKI[2,4], VLADIMIR M. PETRUŠEVSKI[5], KENDE ATTILA BÉRES[2,6], ATTILA FARKAS[7], IMRE MIKLÓS SZILÁGYI[2] and LÁSZLÓ KÓTAI[2,8]*

[1]*Department of Chemistry, Biochemistry and Environmental Protection, Faculty of Sciences, University of Novi Sad, Trg Dositeja Obradovića 3, 21000 Novi Sad, Serbia,* [2]*Institute of Materials and Environmental Chemistry, Research Centre for Natural Sciences, Magyar Tudósok krt. 2., H-1117 Budapest, Hungary,* [3]*Department of Inorganic and Analytical Chemistry, Budapest University of Technology and Economics, Műegyetem rakpart 3, H-1111 Budapest, Hungary,* [4]*Centre for Structural Science, Research Centre for Natural Sciences, Magyar Tudósok krt. 2., H-1117 Budapest, Hungary,* [5]*Faculty of Natural Sciences and Mathematics, Ss. Cyril and Methodius University, Skopje, MK-1000, North Macedonia,* [6]*György Hevesy PhD School of Chemistry, Institute of Chemistry, ELTE Eötvös Loránd University, Pázmány Péter s. 1/A, H-1117 Budapest, Hungary,* [7]*Department of Organic Chemistry and Technology, Budapest University of Technology and Economics, Műegyetem rkp. 3., H-1111, Budapest, Hungary and* [8]*Deuton-X Ltd., Selmeci u. 89, H-2030, Érd, Hungary*

(Received 2 July, revised 11 July, accepted 8 September 2023)

Abstract: Structural and spectroscopic characterization (SXRD, IR, liq. N_2 temperature Raman, UV) of hexaamminecobalt(III) dibromide permanganate, $[Co(NH_3)_6]Br_2(MnO_4)$ (compound **1**), are described. There is a 3D hydrogen bond network including N–H···O–Mn and N–H···Br interactions, which could serve as potential reaction centres for solid-phase redox reactions between the ammonia ligands and/or bromide ions as reductants and permanganate ions as oxidant agents. The effect of the nature of halogen ions on the structural and spectroscopic properties of $[Co(NH_3)_6]Br_2(MnO_4)$ and the analogous chloride compound, $[Co(NH_3)_6]Cl_2(MnO_4)$ (compound **2**), are discussed in detail.

Keywords: permanganate; ammine; cobalt(III); IR and Raman spectroscopy; solid-phase quasi-intramolecular redox reaction.

INTRODUCTION

The preparation and thermal decomposition of transition metal complexes with reducing ligands and oxygen-containing anions are intensively studied areas

* Corresponding author. E-mail: kotai.laszlo@ttk.hu
# Serbian Chemical Society member.
https://doi.org/10.2298/JSC230702062B

of coordination chemistry,[1–5] especially due to the possible quasi-intramolecular redox reactions observed between their reducing ligands and oxidizing anions,[6–10] which result in various simple and mixed nanosized metal oxides, nitrides or alloys.[11–21]

The controlled-temperature thermal decomposition reaction of ammine complexes with permanganate counter ion generally resulted in regular $M^{II}Mn_2O_4$ spinels (M = Cu, Zn, Cd) from divalent and mixed spinels ($M^{II}M^{III}{}_2O_4$, M = = $Co^{II/III}$, $Mn^{II/III}$) from trivalent metals, depending on the decomposition conditions.[6–10] The permanganate salts of the ammonia complexes of cobalt(III) have enormous importance (compound **1**–**3**, Table I) because the mixed Co–Mn oxides formed during their thermal decomposition (*e.g.*, compounds **2**–**4**) were proved to be efficient catalysts in Fischer–Tropsch synthesis and in the photochemical decomposition of toxic dyes (compounds **2** and **4**).[11,12] The Co:Mn mole ratios in the prepared oxides can be adjusted with the Co:permanganate ion ratios in the precursors, *e.g.*, with the use of other counter ions such as carbonate or halides. The presence of halide ions, depending on the chemical form (coordinated or counter-ion) can drastically change the nature of the decomposition products.[12,17] In order to predict the possibility of quasi-intramolecular solid--phase redox reactions, knowing the structural and spectroscopic features of the potential precursors is essential, thus continuing our previous efforts to synthesise, characterise and decompose various halogenide ion-containing ammine complexes of cobalt(III) permanganate,[4,11,12,15,17,21] we have synthesized the poorly characterized hexaamminecobalt(III) dibromide permanganate[22] and discussed its structural and spectroscopic features. The list of compounds used in the evaluation of the properties of compound **1** is given in Table I.

TABLE I. Labels of compounds prepared or evaluated

Compound	Label	Co:Mn ratio	Reference
$[Co(NH_3)_6]Br_2(MnO_4)$	1	1	Present work
$[Co(NH_3)_6]Cl_2(MnO_4)$	2	1	12
$[Co(NH_3)_4CO_3]MnO_4$	3	1	11
$[Co(NH_3)_6](MnO_4)_3$	4	3	12
$[Co(NH_3)_6]Br_3$	5	–	23

EXPERIMENTAL

Chemical-grade cobalt(II) bromide, ammonium bromide, hexachloridoplatinic acid ($H_2PtCl_6{\cdot}6H_2O$), silver nitrate, sodium chromate, or 40, 25 and 37 % aq. sodium permanganate, ammonia and hydrobromic acid solutions, respectively, were supplied by Deuton-X Ltd. (Érd, Hungary).

*Synthesis of compound **1***

Compound **1** was prepared following Klobb's method[22] by a direct combination of 1.00 g of $[Co(NH_4)_3](MnO_4)_3$ and 4.13 g of $[Co(NH_3)_6]Br_3$ in 70 mL of water at 60.0 °C. The mix-

ture was stirred for 15 min and cooled in a refrigerator, where blocks of small strips of crystals were formed at about 1 °C. Then the formed crystals were filtered off and dried in a desiccator at room temperature.

*Preparation of $[Co(NH_3)_6](MnO_4)_3$ (compound **4**) and $[Co(NH_3)_6]Br_3$ (compound **5**)*

$[Co(NH_3)_6]Br_3$ was prepared according to the method of Jörgensen,[23] whereas compound **4** was prepared according to our method.[12]

Analytical methods

The classical analytical and basic instrumental measurements were performed using methods and instruments described in detail in our earlier papers.[1-5] The essential conditions of the measurement methods are listed below.

Elemental analysis. The Co and Mn content of compound **1** was determined by ICP-OES (atomic emission spectroscopy) with a Spectro Genesis ICP-OES instrument (Spectro Analytical Instruments GmbH, Kleve, Germany). A multielement standard (Merck Chemicals GmbH, Darmstadt, Germany) was used for calibration. Bromide content was determined by argentometric titration. The ammonia content was determined by gravimetry in the form of $(NH_4)_2PtCl_6$.

Vibrational spectroscopy. The FT-IR and far-IR spectra of compound **1** were recorded between 4000–400 and 600–100 cm^{-1} ranges in attenuated total reflection (ATR) mode using a BioRad-Digilab FTS-30-FIR and a Bruker Alpha IR spectrometer, respectively.

Raman spectra were measured between 4000 and 200 cm^{-1} on a Horiba Jobin-Yvon LabRAM microspectrometer. An external 532 nm Nd:YAG laser source was used with ~40 mW power and an Olympus BX-40 optical microscope, with an objective of 20× for laser beam focusing. A D2 intensity filter was used to decrease the laser power to 1 %, a confocal hole of 1000 μm, and a monochromator with 1800 groove mm^{-1} (gratings were used for light dispersion). The resolution was 3 cm^{-1}, and the exposure times was 60 s. Due to its sensitivity, the Raman measurement was conducted at 123 K (–150 °C) using a Linkam THMS600 temperature control stage cooled by liquid N_2.

UV–Vis spectroscopy. The room temperature UV–Vis diffuse reflectance spectrum of compound **1** was measured with a Jasco V-670 UV–Vis instrument equipped with an NV-470 integrating sphere ($BaSO_4$ was used as standard).

Powder X-ray diffractometry. Powder X-ray tests were performed with a Philips PW--1050 Bragg–Brentano parafocusing goniometer equipped with a copper cathode (40 kV, 35 mA, secondary beam graphite monochromator, proportional counter). Scans were recorded in the step mode and the diffraction patterns were evaluated with a full profile fitting technique.

Single-crystal X-ray diffraction. A clear red prism-like crystal of $[Co(NH_3)_6]Br_2(MnO_4)$ was mounted on a loop. Cell parameters were determined by the method of least squares using 29943 ($3.080 \leq \theta \leq 30.510$) reflections. Intensity data were collected on a Rigaku R-Axis Rapid diffractometer (monochromator; MoK_α radiation, $\lambda = 0.71073$Å) at 103(2) K. A total of 39290 reflections were collected of which 3727 were unique (R(int) = 0.1132, $R(\sigma) = 0.0438$); intensities of 3309 reflections were greater than $2\sigma(I)$. Completeness to $\theta = 1.000°$. A numerical absorption correction was applied to the data (the minimum and maximum transmission factors were 0.482 and 0.889).

The structure was solved by iterative methods (and subsequent difference syntheses).

Anisotropic full-matrix least-squares refinement on F2 for all non-hydrogen atoms yielded $R_1 = 0.0438$ and $wR_2 = 0.0759$ for 3309 ($I > 2\sigma(I)$) and $R_1 = 0.0531$ and $wR_2 = 0.0783$ for all (3727) intensity data, (number of parameters = 136, goodness-of-fit = 1.188, the max-

imum and mean shift/esd are 0.001 and 0.000, respectively). The maximum and minimum residual electron densities in the final difference map were 0.67 and –0.68 eÅ^{-3}, respectively. The weighting scheme applied was $w=1/(\sigma^2(F_o^2) + (0.0133P)^2 + 3.4263P)$, where $P = (F_o^2 + 2F_c^2)/3$.

Hydrogen atomic positions were calculated from assumed geometries. Hydrogen atoms were included in the structure factor calculation but they were not refined. The isotropic displacement parameters of the hydrogen atoms were approximated from the *U*(eq) value of the atom they were bonded to. CSD Deposition Number is 2277240.

Thermal studies

The DSC curves were recorded between −140 and 25 °C with a Perkin Elmer DSC 7 instrument, with a sample mass of 3–5 mg and a heating rate of 5 °C/min under a continuous nitrogen or oxygen flow (20 cm^3 min^{-1}) in an unsealed aluminium pan.

RESULTS AND DISCUSSION

*Synthesis and properties of compound **1***

Hexaamminecobalt(III) dibromide permanganate (compound **1**) was isolated by Klobb[22] in the reaction (1) of $[Co(NH_3)_6](MnO_4)_3$ (compound **4**) and $[Co(NH_3)_6]Br_3$ (compound **5**) in water at 50 °C in a mole ratio of 1:2:

$$[Co(NH_3)_6](MnO_4)_3 + 2[Co(NH_3)_6]Br_3 \rightarrow 3[Co(NH_3)_6]Br_2(MnO_4) \quad (1)$$

The brilliant purple prisms of compound **1** contrary to the chloride complex (compound **2**) dissolve congruently in water. Repeating the Klobb's experiment, but with concentrated $NaMnO_4$ solution instead of $KMnO_4$ solution, the yield was found to be 84.3 %. The chloride complex (compound **2**) was prepared with 17.6 % yield[12] under similar conditions. The satisfactory yield of compound **1** might be attributed to the higher permanganate concentration in the solution of $NaMnO_4$ than in the concentrated solutions of $KMnO_4$[24] and to the lower solubility of compound **1** (0.32 g/100 mL water) than compound **2** (7.89 g/100 mL of water).[12] Some alternative reaction routes to prepare the permanganate salts[25–28] were also tested but these methods resulted in mixtures of products due to by--reactions of the bromides.

Compound **1** is not soluble in common organic solvents like hexane, benzene, toluene, CCl_4, chloroform, dichloromethane or acetone. $[Co(NH_3)_6]Br_2(MnO_4)$ decomposes at refluxing under xylene (b.p. 140 °C). During the DSC measurement, there was no sign of structural transformation between –140 and 25 °C (Fig. S-1 of the Supplementary material to this paper).

*Structure of compound **1***

Red prismatic single crystals of compound **1** were grown upon slow evaporation of the saturated aqueous solution at room temperature. Some selected crystallographic data of compound **1** based on the refinement results are compared with the data of compound **2** in Table S-I of the Supplementary material.

The structural features of compound **1** are given in Figs. 1–3. The bond distances and angles including the parameters of the hydrogen bond system in compound **1** are given in Tables S-II–S-IV of the Supplementary material. Compound **1** crystallises in the monoclinic system with space group $P2_1/c$ (Nr. 14). The asymmetric unit contains two (different) halves of hexaamminecobalt(III) cation (Fig. 1), and three anions (two bromides and one permanganate). The unit cell contains 4 hexaamminecobalt(III) dibromide permanganate ($Z = 4$).

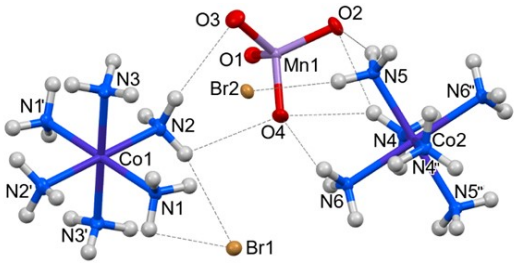

Fig. 1. Structure and labelling of hexaamminecobalt(III) dibromide permanganate, hydrogen bonds are drawn with grey dashed lines (thermal ellipsoids are drawn at the 50 % probability level, symmetry codes to generate equivalent atoms: ': $-x+1,-y+1,-z+1$, ": $-x,-y+1,-z$).

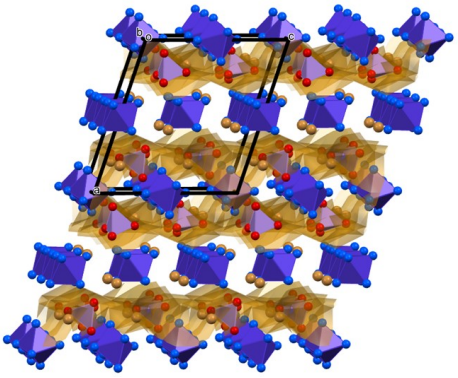

Fig. 2. The unit cell of: $[Co(NH_3)_6]Br_2(MnO_4)$, (polyhedral representation, hydrogen atoms are omitted for clarity, anionic layers are marked with orange shading).

The two different complex cations (labelled as A and B) in compound **1** have distorted octahedral geometries (bond angles ranging between 89.0 and 91.1°, very close to those in compound **2** (89.1 and 91.9°, Fig. 1). Each cation component has three kinds of ammonia ligands. The ammonia ligands in the opposite (axial) positions are equal within both cations A (N1,N1'; N2,N2'; N3,N3') and B (N4,N4"; N5,N5"; N6,N6"). The cations Co–N and anions Mn–O bond distances in compound **1** were found to be 1.957(3)–1.982(3) Å and 1.608–1.627 Å, which values are a little bit shorter than those found in compound **2** (1.949–1.975 Å and 1.605–1.622 Å), respectively.

Direct metal–metal interactions are not present in the structure of compound **1**. The shortest Co–Co, Mn–Mn, and Co–Mn distances are 7.223, 6.922 and 5.032 Å, respectively. The values of 7.198(1), 6.895(1) and 5.011(1) Å were found in compound **2**. The packing arrangement of compound **1** is shown in Fig. 2. The structure is built up of two types of 2D cationic layers in the *bc* plane alternating with anionic layers.

In the first cationic layer, hexaamminecobalt(III) cation A is placed together with Br1 anions whereas the second cationic layer is built up of cation B only (without bromides). The Br2 ions are pushed into the anionic permanganate layers. The anionic permanganate–Br2 layers are in close contact with the cationic B layers. In the layers of cation A, the charge is reduced due to the presence of Br1 anion, and the cation A stays further from the permanganate layers.

A total of 24 hydrogen bonds with various strengths exist between the two kinds of complex cations and the bromideS and permanganates. The ammonia molecules of cation A form three to four and in cation B three to five hydrogen bonds, with the permanganates and bromides. Each bromide has six hydrogen bonds: all the Br1 atom hydrogen bonds are attached to cation A, in addition, two Br1 and four Br2 hydrogen bonds are attached to cation B, too. The Br1 has a bidentate (hydrogen) bonding mode with two ammonia ligands. The cations A and B have 3 and 9 N–H···O (2.937(4)–3.273(4) Å and 2.922(4)–3.243(4) Å) and 8 and 4 N–H···Br (3.402(3)–3.702(3) Å and 3.417(3)–3.704(2) Å) hydrogen bonds, respectively. The summarized number of hydrogen bonds in the cations A and B are equal, 12 in each. The summarized number of hydrogen bonds in the cations A and B are equal, 12 in each. The permanganate oxygens have one bidentate and three tridentate coordination modes. All ammonia ligands of cations A and B are involved in the permanganate hydrogen bonds. The cation A forms altogether 6 hydrogen bonds and the cation B forms 18 hydrogen bonds with the permanganate ions.

The Hirshfeld surface analysis of the two different complex cations supports the structural features characterizing the crystal lattice. The Hirshfeld surface partitions the space between regions where the electron density summed for the atoms of a given molecule surpasses the summed electron density for the remainder of the crystal. 2D fingerprint plots demonstrate best the differences between the two cations. Fingerprint plots were generated for the total interactions of a complex cation and separately for the N–H···O and the N–H···Br interactions. In all cases, the differences are well-marked.

For the cation B, which is embedded in a permanganate anion layer, a spike of N–H···O interactions, marked by the low d_e and d_i values, is visible on the fingerprint plots (Fig. 3d and e) while the spike for the N–H···O interactions for the cation A is missing (Fig. 3b). This shows that while cation *B* has strong interaction with the permanganate anions, cation A is placed further from the

permanganates (the same can also be observed at the H-bond interaction lengths in Table S-III). At the same time, the number of N–H···Br interactions of the cation A is very high (red spike in Fig. 3c). The interaction distances to the bromides, however, are not really different for the two types of cations.

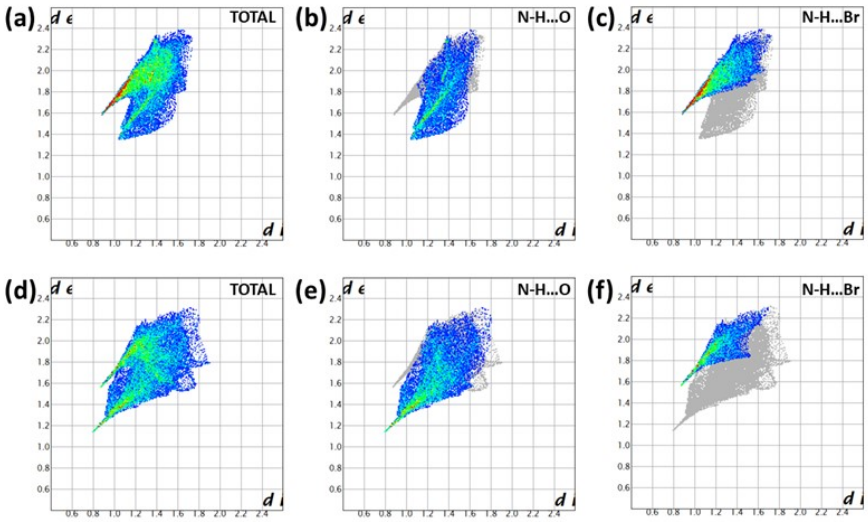

Fig. 3. Fingerprint plots for the two hexaamminecobalt(III) cations: a) total interaction of cation A, b) N–H···O hydrogen bond interactions of cation A, c) N–H···Br hydrogen bonds of cation A, d) intermolecular interactions of cation B, e) NH···O interactions of cation B, f) N–H···Br interactions of cation B; d_i: distance from the Hirshfeld surface to the nearest atom internal to the surface; d_e: distance from the Hirshfeld surface to the nearest atom external to the surface.

*Spectroscopic properties of compound **1***

The factor group analysis results (Figs. 4 and 5), IR and Raman spectra and data (Fig. 6 and Tables II–IV) of compound **1** together with the available spectroscopic data of compound **2** and $[Co(NH_3)_6]^{3+}$have been evaluated in detail.[29–33] The structure of compound **1** in the asymmetric cell was considered to be composed of a central Co^{III} (C_i) cation, two bromides (C_1), six NH_3 molecules (C_1), and one permanganate (C_1). Six (2×3) crystallographically different NH_3 molecules are ligated to the cobalt(III) ion of the two crystallographically different half-cations. Compound **1** is monoclinic ($P2_1/c$) with $Z = 4$, thus a total of 36 internal vibrational modes of the permanganate, 9 of each symmetry species is expected (ν_1 (ν_s) (A) mode, ν_2 (δ_s) (E) mode, and ν_{as} and δ_{as} modes (F_2), respectively, up to 18 bands (9 A_u and 9 B_u) in the IR and the same number (9 A_g and 9 B_g) in the Raman spectra (Fig. 4). The appearance of 12 hindered rotational, and

further 12 hindered translational modes both in the IR (6 A_u and 6 B_u) and Raman (6 A_g and 6 B_g) spectra (Fig. 4) can be expected in the low-frequency part of the spectra.

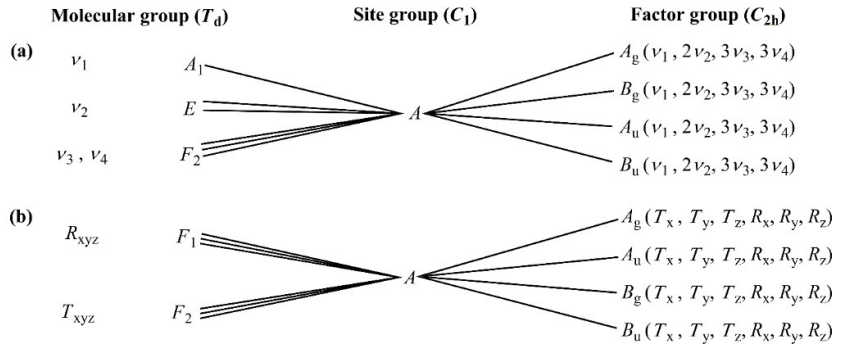

Fig. 4. Internal (a) and external (b) vibrational modes of permanganate ion in compound **1**. ν_1–symmetric stretch.; ν_2–symmetric bend.; ν_3–antisymmetric stretch; ν_4–antisymmetric bend.

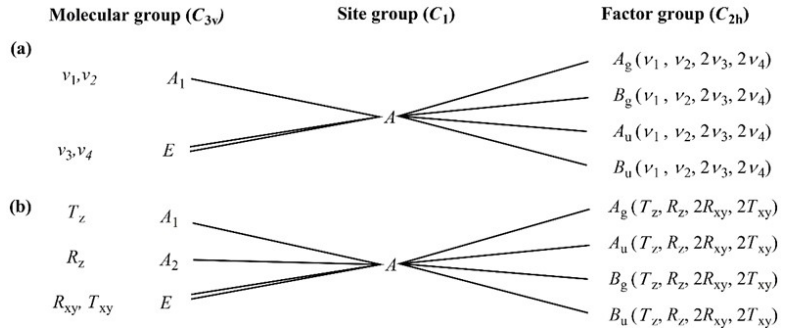

Fig. 5. Internal (a) and external (b) ammonia vibrational modes in compound **1**. ν_1–symmetric stretch.; ν_2–symmetric bend.; ν_3–antisymmetric stretch; ν_4–antisymmetric bend.

Due to the presence of two crystallographically different kinds of Co atoms in compound **1**, the number of translational modes is doubled (2×3 in A_u, and 2×3 in B_u, Fig. S-2).

As the two crystallographically different types of Br ions are at positions of trivial symmetry, the number of modes is also doubled (2×12), thus 6 hindered translations are expected of each symmetry (12 bands in the IR and in the Raman spectra each, Fig. S-3). The six crystallographically different NH_3 molecules are located at positions of trivial symmetry, C_1, thus 12 modes are expected in both the IR (6 A_u and 6 B_u) and the Raman spectra (6 A_g and 6 B_g) (1 ν_1 (ν_s), 1 ν_2 (δ_s) and 2 ν_3 (ν_{as}) and 2 ν_4 (δ_{as}) each) for each crystallographic type of ammonia. The total number of internal vibrations is 6×24 = 144 (Fig. 5). Translations and rotat-

ions along and around an axis, respectively, are given by the lower indices of the axis/axes in question. Due to the six crystallographically different NH_3 molecules, the number of expected modes has to be multiplied by 6, *i.e.*, 6×12 = 72 hindered rotations and 72 hindered translations are expected.

TABLE II. The IR and liq. N_2 temperature Raman spectral data of permanganates in compounds **1** and **2**

Band/assignation	Compound **1**		Compound **2**[12]	
	IR wavenumber, cm^{-1}	Raman shift (532 nm excitation, 130 K) cm^{-1}	IR wavenumber, cm^{-1}	Raman shift (785 nm excitation, 123 K) cm^{-1}
$\nu_1(MnO_4)$, $\nu_s(A)$	834	833	852	843
$\nu_2(MnO_4)$, $\delta_s(E)$	318	348	350	350
$\nu_3(MnO_4)$, $\nu_{as}(F_2)$	922, 896	921,903	924*sh*, 910, 894	927,922,917,912*sh*, 896
$\nu_4(MnO_4)$, $\delta_{as}(F_2)$	388	383	388	398*sh*,393

TABLE III. The IR and liq. N_2 Raman spectral data of the ammonia ligand in compounds **1** and **2**

Band/Assignment	Compound **1**		Compound **2**[12]	
	IR wavenumber, cm^{-1}	Raman shift (532 nm excitation, 130 K) cm^{-1}	IR wavenumber, cm^{-1}	Raman shift (785 nm excitation, 123 K) cm^{-1}
$\rho(NH_3)$	834*	833[a]	813	800
$\delta_s(NH_3)$	1345	325,1310	1340, 1327*sh*	1330, 1323, 1305
$\delta_{as}(NH_3)$	1591	–	1608	–
$\nu_s(NH_3)$	3156	Not measured	3174	Not measured
$\nu_{as}(NH_3)$	3242	Not measured	3256	Not measured

[a]Mixed with $\nu_1(MnO_4)$

TABLE IV. The IR and Raman spectral data of the CoN_6 skeleton in compounds **1** and **2** at 298 K

Band/Assignment	Compound **1**		Compound **2**[12]	
	IR wavenumber, cm^{-1}	Raman shift (532 nm excitation), cm^{-1}	IR wavenumber, cm^{-1}	Raman shift (785 nm excitation), cm^{-1}
$\nu_1(CoN_6)$ ν_s	569, 554, 532*sh*	494	547 (*m*)	507,499
$\nu_2(CoN_6)$ ν_{as}	473,459	-	–	460, 453, 446
$\nu_3(CoN_6)$ ν_s	516, 507, 497,490*sh*	494*	485 (*vw*)	490
$\nu_4(CoN_6)$ δ_{as}	317	323*sh*	317 (*vs*)	320
$\nu_5(CoN_6)$ δ_s		304		311,306
$\nu_6(CoN_6)$ δ	254*sh*	-	254*sh*	–

There are 32 atoms in the formula unit, $Z = 4$, thus it must be multiplied by 4 and by 3 ($3N$, where $N = 32 \times Z = 128$), therefore the total number of rotational

degrees of freedom is altogether 84 (hindered rotations). The total number of internal vibrations and hindered translations in compound **1** is 180 and 120 (72 and 48 for the ammonia ligands and the other parts of the complex), respectively. Three of them are acoustic modes, but the rest (117) are vibrations of translational origin. These give a total number of 384 degrees of freedom.

*Vibrational modes of the permanganate in compound **1***

The IR and Raman spectra of compound **1** are given in Fig. 6 and the band assignments together with those of compound **2** can be seen in Tables II–IV. A singlet symmetric stretching (ν_1), triplet antisymmetric stretching (ν_3) and bending (ν_4) and doublet symmetric deformation (ν_2) modes of permanganates are expected to appear in the IR and Raman spectra. The IR forbidden ν_1 and ν_2 modes are also expected to appear with weak intensities due to the distortion of tetrahedral permanganate ion geometry (Fig. 6).

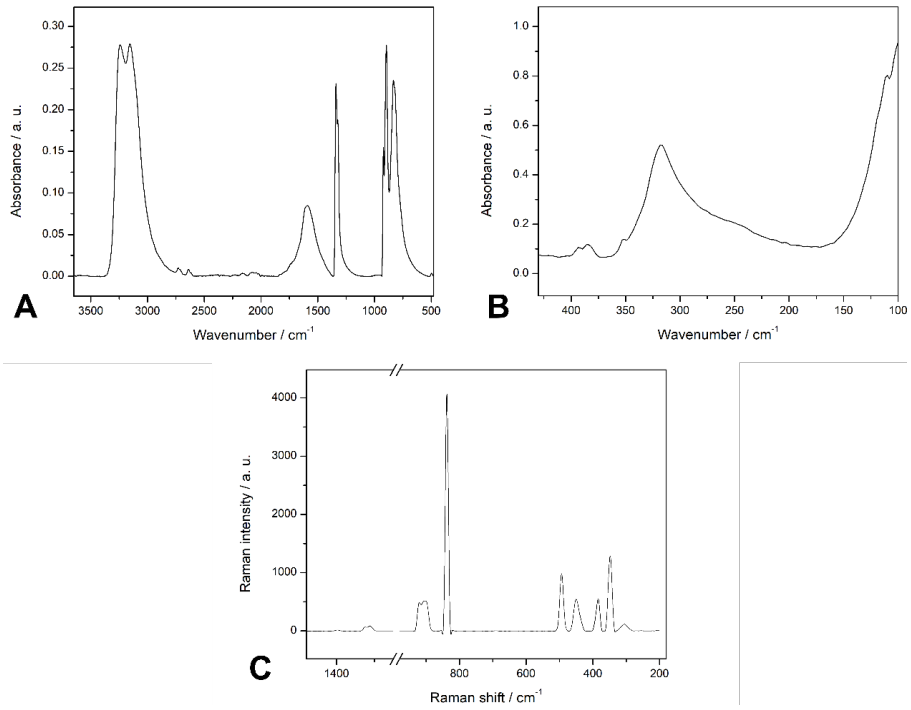

Fig. 6. IR (A), far IR (B) and Raman spectra (C) of compound **1**.

The stretching modes of the permanganate ion in compound **1** appear as a weak singlet at 834 cm^{-1} (ν_s) and as a doublet at 922 and 896 cm^{-1} (ν_{as}), Fig. 6A. The intensity of the band at 834 cm^{-1} shows that the band belongs to the

$\nu_1(MnO_4)$ which is expected to be weak in the IR spectrum and is coinciding with $\rho(NH_3)$. The position of ν_1 is confirmed by the very intense $\nu_1(MnO_4)$ band in the Raman spectrum of compound **1** at 833 cm^{-1} (Fig. 6C) because the $\rho(NH_3)$ is generally weak in the Raman spectra of ammine complexes.[34]

The antisymmetric stretching mode gives the strongest Mn–O band as a doublet in the IR (922, 896 cm^{-1}), and a weak doublet (921, 903 cm^{-1}) in the Raman spectrum of compound **1** (Fig. 6A and C). The two deformation modes of the permanganate ion were found in the far-IR range, δ_s(Mn–O) is a weak band at 318 cm^{-1}, whereas the δ_{as} appeared as a wide band around 388 cm^{-1} (Fig. 6B and C). The IR and Raman bands of permanganate vibrational modes in the IR and Raman spectra of compound **1** are very similar in their positions and intensity to those of the IR and Raman spectra of compound **2**[12] (Table II).

*Vibrational modes of the hexaamminecobalt(III) cation in compound **1***

The correlation analysis of the hexaamminecobalt(III) cation in compound **1** showed two sets of ligand vibrational modes (2×2×3 different ammonia molecules in the two octahedral CoN_6 skeletons). The band assignations of the hexaamminecobalt(III) cation in compound **1** based on normal coordinate analysis, quantum chemical considerations,[29–33] and the recent results on compound **2** are given in Tables III and IV.

The 2×3 crystallographically different NH_3 ligands in each cation type (A and B) resulted in complex band systems for each N–H mode. The band belonging to the symmetric deformation mode appears around 1345 cm^{-1}, thus the relative Co–N bond strength parameter (ε) for the ammonia molecules defined by Grinberg[34] is the same as in compound **2**. Among the vibrational modes belonging to the ammonia ligand, only the rocking mode $\rho(NH_3)$ is sensitive enough to characterise the strength of hydrogen bonds in ammonia complexes.[31] This shows that the average strength of the hydrogen bonds in compound **1** is closer in its strength to $[Co(NH_3)_6]Cl_3$ ($\rho(NH_3)$ = 830 cm^{-1})[31] than that to $[Co(NH_3)_6]Br_3$ ($\rho(NH_3)$ = 830 cm^{-1})[31] or $[Co(NH_3)_6](MnO_4)_3$ ($\rho(NH_3)$ = 803 cm^{-1}).[35]

The CoN_6 octahedron (O_h) has six normal modes, among them three [$\nu_1(\nu(CoN), A_g]$, $\nu_2(\nu_{as}, E_g)$ and $\nu_5(\delta_s, F_{2g})$ are only Raman and two ($\nu_3(\nu_s, F_{1u})$ and $\nu_4(\delta_{as}, F_{1u})$) are only IR active modes. The $\nu_6(\delta(NCoN), F_{2u})$ mode is silent in both IR and Raman spectra. The band positions were determined based on the normal coordinate analysis[29,30,33,36] and the spectroscopic results of compound **2**.[12] The ν_1 mode is singlet, thus the two bands and a shoulder show the separation of $\nu(CoN_6)$ modes in the two different CoN_6 moieties. The well-separated $\nu_3(CoN_6)$ (ν_s) and a singlet of $\nu_4(CoN_6)$ (δ_{as}) appear in the IR spectrum, whereas only three bands, the ν_3–ν_5 modes were found in the Raman spectra. The geometry distortion results in the appearance of the forbidden ν_6 ($\delta(CoN_6)$) band as

well as a shoulder in the IR spectrum around 254 cm^{-1} observed in the IR spectrum of compound **2** as well.[12]

UV–Vis Spectroscopy

The solid phase UV–Vis spectrum of compound **1** can be seen in Fig. S-4. The strongly overlapping absorption bands of four possible d–d transitions of the $[Co(NH_3)_6]^{3+}$ and the CT bands of the permanganate can be observed.[17,37] Co(III) in compound **1** is a low spin cation, the ground state of $[Co(NH_3)_6]^{3+}$ is t_{2g}^6 ($^1A_{1g}$). The excited electron ($t_{2g}^5e_g$) spans with $^3T_{1g}$+$^1T_{1g}$+$^1T_{2g}$+$^3T_{2g}$ terms. The triplet states have lower energies than the singlet ones. As usual, the intensity of spin-allowed transitions (singlet terms) is expected to give weak bands.[38–42] The presence of hydrogen bonds can result in trigonal distortion of the octahedral structure and accordingly to the appearance of new bands.[38] The experimentally found UV–Vis bands' data are given in Table V.

TABLE V. Electronic transitions (in nm) of the hexaamminecobalt(III) cation in compounds **1** and **2** and in octahedral and trigonally distorted (compressed) octahedral structures

Assignment in O symmetry	Assignment in D_3 symmetry	Compound **1**	Compound **2**[12]	$[Co(NH_3)_6]Cl_3$[38]	Calculated DFT (LC-BLYP/6-31G)[38]
$^1A_1 \rightarrow {}^3T_1$	$^1A_1 \rightarrow {}^3E$	805	830	833	806
	$^1A_1 \rightarrow {}^3A_2$				775
$^1A_1 \rightarrow {}^5T_2$	$^1A_1 \rightarrow {}^5E$	676	727	730	740
	$^1A_1 \rightarrow {}^5A_1$				724
$^1A_1 \rightarrow {}^3T_2$	$^1A_1 \rightarrow {}^3E$	600	–	617	613
	$^1A_1 \rightarrow {}^3A_1$	567	575sh	581	585
$^1A_1 \rightarrow {}^1T_1$	$^1A_1 \rightarrow {}^1E$	485	490	486	465
	$^1A_1 \rightarrow {}^1A_2$	419	450	444	459
$^1A_1 \rightarrow {}^1T_2$	$^1A_1 \rightarrow {}^1E$	391	375	367	367
	$^1A_1 \rightarrow {}^1A_1$	352*sh*, 337	343, 330*sh*	324	327

The $^1A_1 \rightarrow {}^1T_1$ and $^1A_1 \rightarrow {}^1T_2$ transitions of the octahedral $Co(NH_3)_6^{3+}$ are spin-allowed, and the hydrogen bonds can cause trigonal distortion (compression) as it was found experimentally in the aq. $[Co(NH_3)_6]Cl_3$ solutions and obtained by the DFT calculations in water–$[Co(NH_3)_6]^{3+}$ systems.[38] The band observed at 253 cm^{-1} as in the case of compound **2** (250 cm^{-1}) may be assigned to the CT band of the cation or to the $^1A_1$–$^1T_2$ ($3t_2$–2e) transition of the permanganate (259 nm for $KMnO_4$). The band at 225 nm (220 nm in the spectrum of compound **2**) may be assigned to the $^1A_1$–$^1T_2$ (t_1–$4t_2$) transition of a permanganate (227 nm for $KMnO_4$).[17] The visible region of the spectrum of compound **1** contains the bands at 510 and 530 nm that might belong to the permanganate $^1A_1$–$^1T_2$ (t_1–2e) transition. The bands at 490 and 551 nm may belong to the permanganate ion. Similar bands were found in the spectrum of $KMnO_4$ at 500 and

562 nm.[17] The band found at 725 nm in the spectrum of compound **2** is shifted to 676 nm, and it probably consists of the $^1A_1$–$^1T_1(t_1$–$2e)$ transition of the permanganate and a component of the $^1A_1 \rightarrow {}^5T_2$ transition of the hexaamminecobalt(III) cation.[12,17] The $^1A_1$–$^1T_1(t_1$–$2e)$ transition of the permanganate was found at 720 nm for $KMnO_4$ and 710 nm for $[Agpy_2]MnO_4$.[2]

In the visible region of spectra, the bands at 510 and 530 nm belong to the permanganate $^1A_1$–$^1T_2$ (t_1–$2e$) transition, whereas the bands at 490 and 551 nm may belong to the permanganate and cation transitions (Table S-VII) as well. A similar band system was found in the UV–Vis spectrum of $KMnO_4$ between 500 and 562 nm.[17] The band at 725 nm is the strongest and probably consists of the $^1A_1$–$^1T_1(t_1$–$2e)$ transition of the permanganate ion and a weak component of the $^1A_1 \rightarrow {}^5T_2$ transition of the complex cation. The $^1A_1$–$^1T_1(t_1$–$2e)$ transition of the permanganate was found at 720 nm for $KMnO_4$ and 710 nm for $[Agpy_2]MnO_4$.[2]

CONCLUSION

We synthesised hexaamminecobalt(III) dibromide permanganate, $[Co(NH_3)_6]Br_2(MnO_4)$ (compound **1**) in the reaction of $[Co(NH_3)_6]Cl_3$ and $[Co(NH_3)_6](MnO_4)_3$. Compound **1** was characterised spectroscopically (FT-IR, far-IR, Raman and UV). Its structure was determined by single-crystal X-ray diffraction. The 3D hydrogen bond network (N–H···O–Mn and N–H···Br interactions) are potential centres of a solid-phase redox reaction between the permanganate and the ammonia ligand. $[Co(NH_3)_6]Br_2(MnO_4)$ decomposes at refluxing under xylene (b.p. 140 °C), thus as a hydrogen bond-containing compound with a low decomposition point is a potential candidate to perform further studies on the existence and reaction products of solid phase heat-induced redox reactions between the cationic and anionic components.

SUPPLEMENTARY MATERIAL

Additional data and information are available electronically at the pages of journal website: https://www.shd-pub.org.rs/index.php/JSCS/article/view/12464, or from the corresponding author on request.

Acknowledgements. The research was supported by the European Union and the State of Hungary, co-financed by the European Regional Development Fund (VEKOP-2.3.2-16-2017--00013) (LK) and the ÚNKP-21-3 and 22-3 New National Excellence Program of the Ministry of Culture and Innovation from the source of the National Research, Development and Innovation Fund (KAB) and the National Research Development and Innovation Office through OTKA grant K124544. BBH thanks the Ministry of Education, Science and Technological Development of the Republic of Serbia (Grant No. 451-03-68/2023-14/200125) for funding.

ИЗВОД

СПЕКТРОСКОПСКА И СТРУКТУРНА КАРАКТЕРИЗАЦИЈА [ХЕКСААММИНКОБАЛТ(III)]-БРОМИД-ПЕРМАНГАНАТА

BERTA BARTA HOLLÓ,[1] NILOOFAR BAYAT,[2,3] LAURA BERECZKI[2,4], VLADIMIR M. PETRUŠEVSKI[5], KENDE ATTILA BÉRES[2,6], ATTILA FARKAS[7], IMRE MIKLÓS SZILÁGYI[2] и LÁSZLÓ KÓTAI[2,8]

[1]Департман за хемију, биохемију и заштиту животне средине, Природно-математички факултет, Универзитет у Новом Сад, Трг Доситеја Обрадовића 3, 21000 Нови Сад, Србија, [2]Institute of Materials and Environmental Chemistry, Research Centre for Natural Sciences, Magyar Tudósok krt. 2., H-1117 Budapest, Hungary, [3]Department of Inorganic and Analytical Chemistry, Budapest University of Technology and Economics, Műegyetem rakpart 3, H-1111 Budapest, Hungary, [4] Centre for Structural Science, Research Centre for Natural Sciences, Magyar Tudósok krt. 2., H-1117 Budapest, Hungary, [5]Faculty of Natural Sciences and Mathematics, Ss. Cyril and Methodius University, Skopje, MK-1000, North Macedonia, [6]György Hevesy PhD School of Chemistry, Institute of Chemistry, ELTE Eötvös Loránd University, Pázmány Péter s. 1/A, H-1117 Budapest, Hungary, [7]Department of Organic Chemistry and Technology, Budapest University of Technology and Economics, Műegyetem rkp. 3., H-1111, Budapest, Hungary, [8]Deuton-X Ltd., Selmeci u. 89, H-2030, Érd, Hungary

У овом раду је описана структурна и спектроскопска карактеризација (дифракција X-зрака на монокристалу, инфрацрвена и Раман спектроскопија на температури течног азота) хексаамминкобалт(III)-бромид-перманганата $[Co(NH_3)_6]Br_2(MnO_4)$ (једињење **1**). Тродимензионална мрежа водоничних веза у једињењу **1** која укључује N–H···O–Mn и N–H···Br интеракције представља потенцијални центар чврстофазне редокс реакције координованог амонијака или бромидних јона као редукујућих и перманганата као оксидујућег агенса. Ефекат природе халогенидног јона на структурна и спектроскопска својства једињења **1**, као и аналогни хлоридни комплекс (једињење **2**) је детаљно дискутован у раду.

(Примљено 2. јула, ревидирано 11. јула, прихваћено 8. септембра 2023)

REFERENCES

1. B. Barta Holló, V. M. Petruševski,G. B. Kovács, F. P. Franguelli, A. Farkas, A. Menyhárd, G. Lendvay, I. E. Sajó, L. Bereczki, R. P. Pawar, E. Bódis, I. M. Szilágyi, L. Kótai, *J. Therm. Anal. Calorim.* **138** (2019)1193 (https://doi.org/10.1007/s10973-019-08663-1)
2. G. B. Kovács, N. V. May, P. A. Bombicz, S. Klébert, P. Németh, A. Menyhárd, G. Novodárszki, V. Petruševski, F. P. Franguelli, J. Magyari, K. Béres, I. M. Szilágyi, L. Kótai, *RSC Adv.* **9** (2019) 28387 (https://doi.org/10.1039/C9RA03230D)
3. K.A. Béres, Z. Homonnay, L. Kvitek, Zs. Dürvanger, M. Kubikova, V. Harmat, F. Szilágyi, Zs. Czégény, P. Németh, L. Bereczki, V.M. Petrusevski, M. Pápai, A. Farkas, L. Kótai, *Inorg. Chem.* **61** (2022) 14403 (https://doi.org/10.1021/acs.inorgchem.2c02265)
4. L. Bereczki, L. A. Fogaca, Zs. Durvanger, V. Harmat, K. Kamarás, G. Németh, B. Barta Holló, V. Petruševski, E. Bódis, A. Farkas, I. M. Szilágyi, L. Kótai, *J. Coord. Chem.* **74** (2021) 2144 (https://doi.org/10.1080/00958972.2021.1953489)
5. V. M. Petruševski, K. A. Béres, P. Bombicz, A. Farkas, L. Kótai, L. Bereczki, *Maced. J. Chem. Chem. Eng.* **41** (2022) 37 (https://doi.org/10.20450/mjcce.2022.2490)
6. F.F. Tao, *Chem. Soc. Rev.* **41** (2012) 7977 (https://doi.org/10.1039/C2CS90093A)
7. L. Kótai, K. K. Banerji, I. Sajó, J. Kristof, B. Sreedhar, S. Holly, G. Keresztury, A. Rockenbauer, *Helv. Chim. Acta* **85** (2002) 2316 (https://doi.org/10.1002/1522-2675(200208)85:8<2316::AID-HLCA2316>3.0.CO;2-A)
8. V. I. Saloutin, Y. O. Edilova, Y. S. Kudyakova, Y. V. Burgart, D. N. Bazhin, *Molecules* **27** (2022) 7894 (https://doi.org/10.3390/molecules27227894)

9. L. Kótai, I. E. Sajó, E. Jakab, G. Keresztury, Cs. Németh, I. Gács, A. Menyhárd, J. Kristóf, L. Hajba, V. Petruševski, V. Ivanovski, D. Timpu, P. L. Sharma, *Z. Anorg. All. Chem.* **638** (2012) 177 (https://doi.org/10.1002/zaac.201100467)
10. I. E. Sajó, L. Kótai, G. Keresztury, I. Gács, Gy. Pokol, J. Kristóf, B. Soptrayanov, V. Petruševski, D. Timpu, P.K. Sharma, *Helv. Chim. Acta* **91** (2008) 1646 (https://doi.org/10.1002/hlca.200890180)
11. M. Mansouri, H. Atashi, F. F. Tabrizi, A. A. Mirzaei, G. Mansouri, *J. Ind. Eng. Chem.* **19** (2013) 1177 (https://doi.org/10.1016/j.jiec.2012.12.015)
12. L. Bereczki, V. M. Petruševski, F. P. Franguelli, K. A. Béres, A. Farkas, B. Barta Holló, Zs. Czégény, I. M. Szilágyi, L. Kótai, *Inorganics* **10** (2022) 252 (https://doi.org/10.3390/inorganics10120252)
13. R. N. Mehrotra, *Inorganics* **11**(2023), 308 (https://doi.org/10.3390/inorganics11070308)
14. L. A. Fogaça, L. Bereczki, V. M. Petruševski, B. Barta Holló, F. P. Franguelli, M. Mohai, K. A. Béres, I. E. Sajó, I. M. Szilágyi, L. Kotai, *Inorganics* **9** (2021) 38 (https://doi.org/10.3390/inorganics9050038)
15. F. P. Franguelli, B. Barta Holló, V. M. Petruševski, I. E. Sajó, S. Klébert, A. Farkas, E. Bódis, I. M. Szilágyi, R. P. Pawar, L. Kótai, *J. Therm. Anal. Calorim.* **145** (2021) 2907 (https://doi.org/10.1007/s10973-020-09991-3)
16. K. A. Béres, I. E. Sajó, G. Lendvay, L. Trif, V. M. Petruševski, B. Barta Holló, L. Korecz, F. P. Franguelli, K. László, I. M. Szilágyi, L. Kótai, *Molecules* **26** (2021) 4022 (https://doi.org/10.3390/molecules26134022)
17. F. P. Franguelli, É. Kováts, Zs. Czégény, L. Bereczki, V. M. Petruševski, B. Barta Holló, K. A. Béres, A. Farkas, I. M. Szilágyi, L. Kótai, *Inorganics* **10** (2022) 18 (https://doi.org/10.3390/inorganics10020018)
18. L. A. Fogaca, É. Kováts, G. Németh, K. Kamarás, K. A. Béres, P. Németh, V. Petruševski, L. Bereczki, B. Barta Holló, I. E. Sajó, I. M. Szilágyi, L. Kótai, *Inorg. Chem.* **60** (2021) 3749 (https://doi.org/10.1021/acs.inorgchem.0c03498)
19. H. E. Solt, P. Németh, M. Mohai, I. E. Sajó, S. Klébert, F. P. Franguelli, L. A. Fogaca, R. P. Pawar, L. Kótai, *ACS Omega* **6** (2021) 1523 (https://doi.org/10.1021/acsomega.0c05301)
20. K. A. Béres, Z. Homonnay, B. Barta Holló, M. Gracheva, V. M. Petruševski, A. Farkas, Zs. Dürvanger, L. Kótai, *J. Mater. Res.* **38** (2023) 1102 (https://doi.org/10.1557/s43578-022-00794-w)
21. K. A. Béres, F. Szilágyi, Z. Homonnay, Zs. Dürvanger, L. Bereczki, L. Trif, V. M. Petruševski, A. Farkas, N. Bayat, L. Kótai, *Inorganics* **11** (2023) 68 (https://doi.org/10.3390/inorganics11020068)
22. T. Klobb, *Bull. Soc. Chim.* **47** (1887) 240
23. S. M. Jörgensen, *J. Prakt. Chem.* **35** (1887) 417
24. L. Kótai, L. Gács, I. E. Sajó, P. K. Sharma, K. K. Banerji, *Trends. Inorg. Chem.* **11** (2011) 25 (10.1002/chin.201113233)
25. L. Kótai, I. E. Sajó, I. Gács, K. S. Pradeep, K. K. Banerji, *Z. Anorg. All. Chem.* **633** (2007) 1257 (https://doi.org/10.1002/zaac.200700142)
26. L. Kótai, K. K. Banerji, *Synth. React. Inorg. Met. Org. Chem.* **31** (2001) 491 (https://doi.org/10.1081/SIM-100002234)
27. L. Kótai, A. Keszler, J. Pató, S. Holly, K. K. Banerji, *Ind. J. Chem., A* **38** (1998) 966 (https://nopr.niscpr.res.in/handle/123456789/15865)
28. T. Klobb, *Bull. Soc. Chim. Paris* **25** (1901) 1022 (https://www.persee.fr/doc/bulmi_0366-3248_1901_num_24_5_2591)

29. Y. Chen, D. H. Christensen, G. O. Sorensen, O. F. Nielsen, E. B. Pedersen, *J. Mol. Struct.* **299** (1993) 61 (https://doi.org/10.1016/0022-2860(93)80283-2)
30. C. Téllez, *Semin., Ciênc. Exatas Tecnol.* **3** (1982) 185 (http://dx.doi.org/10.5433/1679-0367.1982v3n11p185)
31. K. H. Schmidt, A. Müller, *J. Mol Struct.* **22** (1974) 343 (https://doi.org/10.1016/0022-2860(74)85004-0)
32. B. L. Sacconi, A. Sabatini, P. Cans, *Inorg. Chem*. **3** (1964) 1772 (https://doi.org/10.1021/ic50022a026)
33. H. Block, *Trans. Faraday Soc.* **55** (1959) 867 (https://doi.org/10.1039/TF9595500867)
34. A. A. Grinberg, Y. S. Varshavskii, *Primen. Molekul. Spektr. Khim.* **0** (1966) 104
35. E. J. Baran, P. J. Aymonino, *Z. Anorg. Allg. Chem.* **362** (1968) 215 (https://doi.org/10.1002/zaac.19683620312)
36. W. Kiefer, H. J. Bernstein, *Mol. Phys.* **23** (1972) 835 (https://doi.org/10.1080/00268977200100841)
37. P. Hendry, A. Ludi, *Adv. Inorg. Chem.* **35** (1990) 117 (https://doi.org/10.1016/S0898-8838(08)60162-2)
38. H. Sakiyama, Y. Ishiyama, H. Sugawara, *Spectrosc. Lett.* **50** (2017) 111 (https://doi.org/10.1080/00387010.2017.1295272)
39. R. Benedix, H. Hennig, C. Nieke, *Inorg. Chim. Acta* **172** (1990) 109 (https://doi.org/10.1016/S0020-1693(00)80458-2)
40. Y. Mitsutsuka, I. Kondo, M. Nakahara, *Bull. Chem. Soc. Japan* **59** (1986) 2767 (http://pascal-francis.inist.fr/vibad/index.php?action=getRecordDetail&idt=8207253)
41. R. B. Wilson, E. I. Solomon, *J. Am. Chem. Soc.* **102** (1980) 4085 (https://doi.org/10.1021/ja00532a018)
42. R. B. Wilson, E. I. Solomon, *Inorg. Chem.* **17** (1978) 1729 (https://doi.org/10.1021/ja0286371).